

Analysis of a Doubly Fed Induction Generator through Experimental Verification

Milkias Berhanu Tuka, Roberto Leidhold, Mengesha Mamo

Abstract—Experimentation is very important, mainly for the determination of machine parameters like stator and rotor resistances, leakage, self and mutual inductances of the Doubly-Fed Induction Generator (DFIG) which are used in modelling and simulations. These parameters are sometimes difficult to get directly from the nameplate as they are manufacturer (company) secrets in most cases. The parameters of a machine can say a lot about its overall performance behaviors. In addition, experimentation can support and prove simulation results. Thus, the work carried out on a 1kW DFIG in this study analysis its performance under various conditions. The given machine has five rotor positions. Hence the impacts of the rotor at these five positions have been investigated. With the aid of simulation and experimental results, variations of torque, stator current and power, efficiency, and power factor have been investigated with regard to the mechanical output of the machine. The simulation & experimentation encompasses the machine side converter (MSC) for controlling. Comparisons of simulation and experimental results have been done and confirm the validity of analysis with some small deviations.

Keywords—Current Controller, DFIG, MATLAB-Simulink

I. BACKGROUND

Induction machines can work as motors and generators. Doubly Fed Induction Machines (DFIM) as generators, nowadays are getting more popularity in areas like wind turbine applications. Thus, this study focuses on the DFIM operating as a generator. They provide power to the grid, both through the stator and rotor windings depending on the sign of the slip or in other words, super synchronous and sub synchronous mode of operation.

A three-phase wound rotor induction machine that is operating as a Doubly-Fed Induction Generator (DFIG), where the power delivery takes place through the stator and rotor can be referred as simply a doubly-fed induction generator [1]. The DFIG is double-fed; the stator windings are supplied directly by the grid voltage or constant voltage source and the rotor windings have a voltage impressed on them by the rotor converter. Since the stator windings are connected to the grid, the flux is mainly determined by the voltage and frequency of the grid. The applied rotor voltage (v_r) in a DFIG can be adjusted to get the desired slip or torque responses.

The authors are with Otto-Von-Guericke University, Magdeburg, Germany

The frequency of the converter will depend on the slip speed. It is also possible to control power factor or reactive power in the stator circuit similar to a synchronous generator [2], [3]. The size of the machines varies from small watt to megawatt ranges. Sometimes, it is challenging and difficult to conduct laboratory experiments on megawatt generators in educational institutions. Under such circumstances, it is reasonable to conduct experimentation on small size generators and predict the performance of larger ones based on experimental and simulations results.

The equivalent circuit of the induction machine can be drawn as shown in Fig.1 [4].

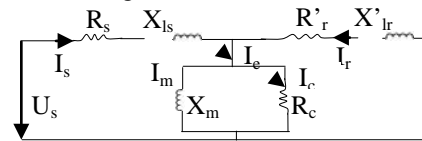


Fig. 1 Equivalent circuit diagram

Where, R_s = per-phase stator resistance, R_r' = per-phase rotor resistance referred to stator side, X_m =per-phase stator magnetizing reactance, R_c = per-phase stator core loss resistance, X_{ls} = stator leakage reactance, U_s = stator voltage, I_s = stator current, I_e = exciting current, I_m = magnetizing current, I_c = core current and I_r = rotor current. The voltage across the magnetizing branch is $U_m = U_s - R_s I_s - I_s j\omega_s L_s$

II. PARAMETERS DETERMINATION DFIG

In order to carry-out various analyses on DFIG, determination of its parameters is very important. Some of the parameters may be obtained from the name plate and others can be determined by performing tests: DC resistance, No load (open circuit), and blocked rotor (short circuit). In this study, the experimentation is carried out on a 1 kW DFIG is shown in Fig. 2 coupled with other machines.



Fig. 2 DFIG under experimentation and other accessories Where, SQIM and PMSG stand for Squirrel Cage Induction Motor and Permanent Magnet Synchronous Generator.

A. DC Resistance Test

The stator and rotor resistances are measured by means of a DC voltage supply. For the machine under study, it can be

reminded that the stator windings are connected to wye and the rotor in the delta. For the purpose of parameter identification, the star equivalence is assumed and used in the analysis.

In some cases, it is required to create a neutral reference for an ungrounded system. Since the rotor of the machine is in delta connected, there is no wye point available for connection to ground. Thus, the artificial ground is created and used.

The measured values for stator winding are given table I.

DC Voltage U_{dc} (V)	DC Current I_{dc} (A)	DC Resistance(Ω); $R_{dc}=U_{dc}/I_{dc}$	AC Resistance $R_{ac}=R_{dc}/2(\Omega)$
5.223	0.356	14.659	7.33

Assuming a balanced system of star equivalent [5]:

$$R_s = \frac{1}{2} \frac{U_{dc}}{I_{dc}} \quad (1)$$

Thus, stator resistance, $R_s = 0.5 * 14.659 \sim 7.33 \Omega$

For rotor winding, the measured results are given in table II.

DC Voltage U_{dc} (V)	DC Current I_{dc} (A)	Dc Resistance(Ω); $R_{dc}=U_{dc}/I_{dc}$	AC Resistance $R_{ac}=R_{dc}/2(\Omega)$
5.330	1.333	4.002	2.001

$$R_r = \frac{1}{2} \frac{U_{dc}}{I_{dc}} \quad (2)$$

Thus, $R_r = 0.5 * 4.002 \sim 2 \Omega$

Since the DFIG under test has 5 rotor positions to enable the controllability at several of its positions, hence it is also important to know the values of resistances at these positions. Following similar measurement procedures, the test results for rotor resistances at 5 rotor positions are displayed in table III.

Rotor Positions	DC Voltage, U_{dc} (V)	DC Current, I_{dc} (A)	Dc Resistance(Ω), $R_{dc}=U_{dc}/I_{dc}$	AC Resistance $R_{ac}=R_{dc}/2(\Omega)$
0	5.662	0.002	infinite	infinite
1	5.636	1.015	5.551	2.776
2	5.092	1.969	2.586	1.293
3	2.169	1.979	1.096	0.548
4	0.059	1.920	0.032	0.016

B. Open Circuit (No Load) Test

For the equivalent circuit diagram of Fig.1, its simplified diagram to conduct open circuit test can be re-drawn as shown in Fig. 3 where there are no current flows in the secondary circuit during no-load operation.

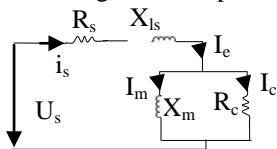


Fig.3. Equivalent circuit diagram at no load test

The magnetizing reactance, X_m and the core resistance, R_c can now be calculated using Fig. 3 and measured values [6].

$$P_{nl} = \sqrt{3} V_{nl} \cdot I_{LL} \cdot \cos \phi_{nl} \quad (3)$$

The measurement results of the open and short circuit tests are given in table IV.

Test	Line-line voltage(V)	I_{nl} (A)	P_{nl} (W)	Speed (rpm)
Open (No load)	404.8V	1,995	156.1	1420

Blocked (Short circuit)	U_{br} (V)	I_{br} (A)	P_{br} (W)	
	183.1	2.8	368.28	0

Where nl stands for no load and br for the blocked rotor.

Using (3), the no load power factor is:

$$\cos \phi_{nl} = \frac{156.1}{\sqrt{3} * 404.8 * 1.995} = 0.112 \rightarrow \phi_{nl} = \cos^{-1}(0.112) = 83.6^{\circ}$$

$$i_c = i_{nl} * \cos \phi_{nl} = 1.995 * 0.112 = 0.223A$$

$$i_m = i_{nl} * \sin \phi_{nl} = 1.995 * \sin(83.6^{\circ}) = 1.98A$$

The no load impedance (Z_{nl}):

$$Z_{nl} = U_{nl} / I_{nl} = 404.8 / \sqrt{3} * 1.995 = 117.15 \Omega$$

Hence the no load resistance (R_{nl}):

$$R_{nl} = Z_{nl} \cos \phi_{nl} = 117.15 * 0.112 = 13.12 \Omega \quad \text{or}$$

$$R_{nl} = \frac{P_{nl}}{3 * I_{nl}^2} = \frac{156.1}{3 * 1.995^2} = 13.1 \Omega$$

$$X_{nl} = Z_{nl} * \sin(\phi_{nl}) = 117.15 * \sin(83.6^{\circ}) = 116.42 \Omega \quad \text{or}$$

$$X_{nl} = \sqrt{(Z_{nl}^2 - R_{nl}^2)} = \sqrt{(117.15^2 - 13.12^2)} = 116.41 \Omega$$

The voltage across magnetising branch (U_m):

$$U_m = U_{s,nl} - I_{s,nl} (R_s + jX_{ls}) = \frac{404.8}{\sqrt{3}} - 1.995(7.33 + j17.2)$$

$$= 219.1 - j34.31V = 216.4 < -8.9^{\circ} V$$

$$R_c = \frac{U_m}{i_c} = \frac{216.4}{0.223} = 970.4 \Omega$$

$$X_m = \frac{U_m}{i_m} = \frac{216.4}{1.98} = 109.3 \Omega$$

$$L_m = \frac{X_m}{2\pi f_s} = \frac{109.3}{2\pi * 50} = 0.3499H \approx 350mH$$

Where, f_s stand for supply frequency.

C. Short Circuit Test

To reach the short circuit test, the torque was kept at maximum value and the rotor was shorted so that it was not rotating and hence the results obtained are shown in table IV. This test is very important to determine the leakage and self-reactance of the machine which is not easily obtained from the manufacturer in most cases. From the short circuit test, the remaining parameters can be calculated as [6]:

$$Z_{br} = \frac{U_{br}}{\sqrt{3} I_{br}} = \frac{183.1}{\sqrt{3} * 2.8} = 37.75 \Omega$$

$$P_{br} = \sqrt{3} V_{br} \cdot I_{LL} \cdot \cos \phi_{br}$$

$$\cos \phi_{br} = \frac{368.28}{\sqrt{3} * 183.1 * 2.8} = 0.415 \rightarrow \phi_{br} = \cos^{-1}(0.415) = 65.5^{\circ}$$

$$R_{br} = Z_{br} \cos \phi_{br} = 37.75 * 0.415 = 15.67 \Omega \quad \text{or}$$

$$R_{br} = \frac{P_{br}}{3 * I_{br}^2} = \frac{368.28}{3 * 2.8^2} = 15.66 \Omega$$

$$X_{br} = Z_{br} * \sin(\phi_{br}) = 37.75 * \sin(65.5^{\circ}) = 34.4 \Omega \quad \text{or}$$

$$X_{br} = \sqrt{Z_{br}^2 - R_{br}^2} = \sqrt{37.8^2 - 15.7^2} = 34.4 \Omega$$

$$X_{ls} \approx X'_{lr} = \frac{X_{br}}{2} = 17.2 \Omega$$

Depending on the design of the machine, different criteria exist to establish the values of L_{ls} and L_{lr} . In general, equal leakage inductances can be assumed [7].

$$L_{ls} = L'_{lr} \approx \frac{X_{ls}}{2\pi f_s} = \frac{17.2}{2\pi * 50} = 0.05475H = 54.75mH$$

$$\text{and} \quad L_{lr} = L'_{lr} / k^2 = 54.75 / 3.2^2 = 5.35 \text{ mH}$$

Where, k is transformation ratio with value 3.2.

III. GAIN CALCULATION OF THE DFIG

The proportional gain (K_p) is given as, $K_p = L / (2T_{\Sigma})$, $T_{\Sigma} = 1.5T_s$ [8]. The switching frequency (f_{sw}) of Guash inverter used under study is 10 kHz and the sampling frequency (f_s) is twice of f_{sw} , i.e., $f_s = 2f_{sw} = 20$ kHz. Then, $T_s = 1/f_s = 50\mu s$ and $T_{\Sigma} = 75\mu s$

$$K_p = \frac{L}{2T_{\Sigma}} = \frac{L_{lr} + L_{ls}}{2T_{\Sigma}} = \frac{2L_{lr}}{2T_{\Sigma}} = \frac{5.35 * 10^{-3}}{75 * 10^{-6}} = 71.33$$

$$T_i = \frac{L}{R} = \frac{L_{lr} + L_{ls}}{R_r + R_s} = \frac{2 * 5.35 * 10^{-3}}{2 + \frac{7.33}{3.2^2}} = 0.00394s = 3.94ms$$

Where, T_{Σ} is the non-compensable time delay, T_i is the integral time constant, and T_s is switching time period.

$$X_s = X_r' = X_{ls} + X_m = 17.2 + 97.42 = 114.62 \Omega$$

Where X_s and X_r' are self-reactance of stator and rotor.

IV. MODELING THE DOUBLY FED INDUCTION GENERATOR

A dynamic model of DFIG can be set up in the form of the two-phase dq-representation there by the complexity of the three-phase differential equations, where some of the machine inductances which are functions of the rotor speed and the time varying voltage equations are avoided. In developing the dynamic model of the DFIG, space vector theory is applied to the basic electric equations of the machine [7]. In connection, by using the known Clarke and its inverse transformations, the three-phase (ABC) quantities can be converted into two stationary frames $\alpha\beta$ quantities and vice versa. The RMS value of grid voltage in $\alpha\beta$ can be used to find out grid voltage angle, ϕ_g [9].

In this way, the general voltage equation is:

$$V = I.R + \frac{d|\psi|}{dt} \quad (4)$$

In stationary reference frame:

$$V_s^s = I_s^s R_s + \frac{d\psi_s^s}{dt} \Rightarrow \begin{cases} v_{\alpha s} = r_s i_{\alpha s} + \frac{d\psi_{\alpha s}}{dt} \\ v_{\beta s} = r_s i_{\beta s} + \frac{d\psi_{\beta s}}{dt} \end{cases} \quad (5)$$

Writing the rotor voltage in stator reference frame:

$$v_r^s = \begin{cases} v_{\alpha r} = R_r i_{\alpha r} + \frac{d\psi_{\alpha r}}{dt} + \omega_m \psi_{\beta r} \\ v_{\beta r} = R_r i_{\beta r} + \frac{d\psi_{\beta r}}{dt} - \omega_m \psi_{\alpha r} \end{cases} \quad (6)$$

In the same way, the stator & rotor flux expressions in space vector form in a stationary reference frame:

$$\begin{bmatrix} \psi_s^s \\ \psi_r^s \end{bmatrix} = \begin{bmatrix} L_s & L_m \\ L_m & L_r \end{bmatrix} \cdot \begin{bmatrix} i_s^s \\ i_r^s \end{bmatrix} \rightarrow \begin{cases} \psi_{\alpha s} = L_s i_{\alpha s} + L_m i_{\alpha r} \\ \psi_{\beta s} = L_s i_{\beta s} + L_m i_{\beta r} \\ \psi_{\alpha r} = L_m i_{\alpha s} + L_r i_{\alpha r} \\ \psi_{\beta r} = L_m i_{\beta s} + L_r i_{\beta r} \end{cases} \quad (7)$$

Taking the inverse Laplace transform:

$$\begin{bmatrix} i_s^s \\ i_r^s \end{bmatrix} = \frac{1}{L_m^2 - L_s L_r} \begin{bmatrix} -L_r & L_m \\ L_m & -L_s \end{bmatrix} \begin{bmatrix} \psi_s^s \\ \psi_r^s \end{bmatrix} \quad (8)$$

Where, $L_s = L_{ls} + L_m$ and $L_r = L_{lr} + L_m$

$v_{\alpha s}$, $v_{\beta s}$, $v_{\alpha r}$, $v_{\beta r}$, $i_{\alpha s}$, $i_{\beta s}$, $i_{\alpha r}$, $i_{\beta r}$ and $\psi_{\alpha s}$, $\psi_{\beta s}$, $\psi_{\alpha r}$, $\psi_{\beta r}$ are voltages [V], currents [A] and flux linkages [Wb] of the stator and rotor in α and β -axis, L_s , L_r , L_m are the stator, rotor and mutual inductances [H]. L_{ls} , L_{lr} are the stator and rotor leakage inductances [H], ω , ω_m are the speed of the reference frame and mechanical angular velocity of the generator rotor [rad/s]. On other hand, stator active and reactive powers are given as:

$$P_s = \frac{3}{2} (v_{\alpha s} i_{\alpha s} + v_{\beta s} i_{\beta s}); \quad Q_s = \frac{3}{2} (v_{\beta s} i_{\alpha s} - v_{\alpha s} i_{\beta s}) \quad (9)$$

While the electromagnetic torque, created by the DFIG is:

$$T_{em} = \frac{3}{2} p \text{Im} \{ \bar{\psi}_r \bar{i}_r \} = \frac{3}{2} p (\psi_{\beta r} i_{\alpha r} - \psi_{\alpha r} i_{\beta r}) \quad (10)$$

By adding the mechanical motion equation that describes the rotor speed behaviour neglecting damping losses:

$$T_{em} + T_m = J \frac{d\omega_m}{dt} \quad (11)$$

Where J is the inertia of the rotor and T_m is the load torque.

The dq voltage equations can be given as: [4], [7]

$$v_{ds} = R_s i_{ds} + \frac{d\psi_{ds}}{dt} - \omega_s \psi_{qs}; \quad v_{qs} = R_s i_{qs} + \frac{d\psi_{qs}}{dt} + \omega_s \psi_{ds} \quad (12)$$

$$v_{dr} = R_r i_{dr} + \frac{d\psi_{dr}}{dt} - \omega_r \psi_{qr}; \quad v_{qr} = R_r i_{qr} + \frac{d\psi_{qr}}{dt} + \omega_r \psi_{dr} \quad (13)$$

$$\psi_{ds} = L_s i_{ds} + L_m i_{dr}; \quad \psi_{qs} = L_s i_{qs} + L_m i_{qr} \quad (14)$$

$$\psi_{dr} = L_m i_{ds} + L_r i_{dr}; \quad \psi_{qr} = L_m i_{qs} + L_r i_{qr}$$

The instantaneous active and reactive powers of a DFIG in a synchronously rotating d-q reference frame are given by:

$$P_s = \frac{3}{2}(v_{ds}i_{ds} + v_{qs}i_{qs}); \quad Q_s = \frac{3}{2}(v_{qs}i_{ds} - v_{ds}i_{qs}) \quad (15)$$

Based on the above models, the masked MATLAB-Simulink block diagram is shown in Fig. 5.

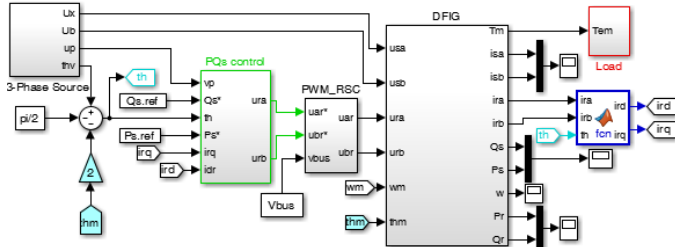


Fig. 5. Masked MATLAB-Simulink Model

V. ANALYSIS OF DOUBLY FED INDUCTION MACHINE

Using the various DFIM equations, the machine can be analysed for generating mode of operation.

A. Doubly Fed Induction Machine as a Generator

This section analyses the performance of DFIM operating as a generator. Table V shows its measurement performance characteristics where T, N, Ps, Qs, Ur, Ir, Pr, PF, S and eff. stands for torque, speed, stator active power, stator reactive power, rotor voltage, rotor current, rotor power, power factor, slip, and efficiency respectively. It is seen that the machine starts to generate power above 1500rpm (synchronous speed) and generates around 10.6W at 1.6Nm torque. When the driving torque increases above 1.2Nm, the DFIG starts to generate more power. This torque overcomes the inertia and friction of the rotor and other components such as bearings.

Table V: Measurement results DFIG

T (Nm)	N (rpm)	Is(A)	Ps (W)	Qs (VAR)	Ur(V)	Ir (A)	Pr (W)	PFs	S	eff.(%)
0.6	-1432	1.95	523.43	584.63	2	0.75	1.71	0.67	0.05	-17.12
1.2	-1402	1.96	364	1305	2.6	1.04	2.84	0.7	0.07	-48.00
1.6	-1554	2.05	-10.61	1409	1.7	0.6	1.25	0.5	-0.04	4.56
2	-1578	2.08	-38.9	1432	2.2	0.68	1.6	0.61	-0.05	12.26
3	-1622	2.18	-147.5	1486	3.3	1.25	4.45	0.4	-0.08	29.83
3.5	-1650	2.24	-210	1522	1.58	4.1	6.6	0.36	-0.10	35.83
4	-1666	2.3	-265	1557	1.94	5.2	10.6	0.34	-0.11	39.51
4.5	-1691	2.35	-331	1594	6	2.22	13.6	0.31	-0.13	43.27
5	-1710	2.42	-371.1	1625	6.6	2.5	17.1	0.29	-0.14	43.38
6	-1750	2.58	-479.7	1705.4	8.1	3.1	28	0.25	-0.17	46.19
7	-1792	2.73	-580	1800	9.8	3.56	36.5	0.21	-0.19	46.96
8	-1836	2.92	-691	1888	11.4	4.16	47.8	0.19	-0.22	48.06
9.1	-1881	3.1	-793	2001	13.2	4.78	63	0.16	-0.25	47.78
10	-1915	3.31	-881	2140	14.4	5.28	76.6	0.15	-0.28	47.78

Furthermore, it can be observed that both the active and reactive power outputs from the DFIG are increasing linearly with the torque. By applying the motor rule, negative power represents generating power and positive power represents energy consumption. Due to its direct relationship, the stator current increases as the machine torque grow up.

Increasing the torque will generate more active power, and meanwhile, the generator will need to consume more reactive power. Without a capability of regulating its reactive power

output, the DFIG will operate at a higher power output with lower power factor but better energy efficiency. Similarly, the rotor current increase with the torque as it is controlled by the quadrature component of the rotor current (10).

At higher power output with increased torque, the slip is negative maximum and power factor is decreasing. The mechanical power in this case is higher than the stator power. To achieve higher speed at higher torque and wind speed as in the case of Wind Turbine Generator (WTG), the machine should have an inverter connected to the rotor circuit to adjust the speed and control action should also play a role as will be discussed in the subsequent sections.

When the load torque increases, the stator current and rotor current goes beyond the rated value which may result in damage to the machine. The maximum stator power at rated stator current (2.9A) when the rotor is at its higher position (2.77Ω) is near 691W and rotor power is 47.8W. Hence, the total power to the grid is 740W. One can notice that, when the slip is at 30%, the power to the grid is near 958W. The maximum efficiency of the machine when operating as a generator in this case is 48.1%. There are also changes in the efficiency of the DFIG as the rotor position varies. It is better at lower rotor resistance as shown in Fig. 6.

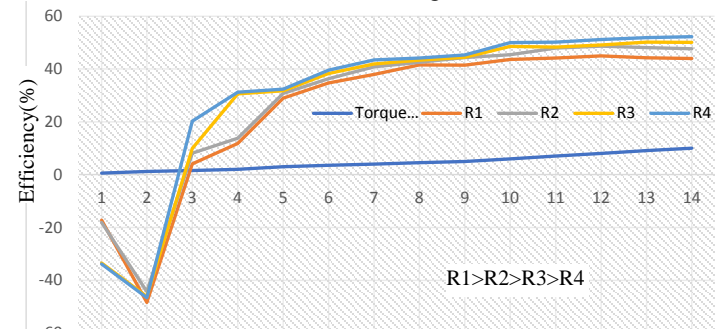


Fig. 6 Efficiency curve of DFIG for rotor position change

Thus, the addition of higher rotor resistance and /or the Pulse Width Modulator (PWM) power converters which are commonly used to allow the power flow back and forth in the DFIG rotor windings can increase the efficiency of the machine as seen in a simulation. Since the first option results in higher losses, the converter option can be recommended for better efficiency and control flexibility.

VI. VECTOR CONTROL OF DFIG

In a vector control of DFIG, the components of the d and q axis of the rotor current are regulated. A reference frame orientated with the stator flux is used for the control of Machine Side Converter (MSC). The active and reactive power flows of the stator can be controlled independently by means of the quadrature and direct currents respectively [7], [10]. Under the rotor current control mode, the stator flux is:

$$\psi_s = L_s i_{ds} + L_m i_{dr} = \psi_{ds}; \quad \psi_{qs} = L_s i_{qs} + L_m i_{qr} = 0 \quad (16)$$

$$i_{ds} = \frac{\psi_s - L_m}{L_s} i_{dr} \quad \text{and} \quad i_{qs} = -\frac{L_m}{L_s} i_{qr} \quad (17)$$

In steady state, the stator flux is proportional to the grid voltage, V_g . Neglecting the small drop in the stator resistance [10], [11]:

$$V_{ds}=0; \quad V_{qs}=V_g \approx \omega_s \psi_s \quad (18)$$

Thus, the stator active and reactive power flow is given as:

$$P_s = -1.5 \hat{V}_g \frac{L_m}{L_s} i_{qr}; Q_s = 1.5 \hat{V}_g \left[\frac{\psi_s}{L_s} - \frac{L_m}{L_s} i_{dr} \right] = 1.5 \hat{V}_g \left[\frac{\hat{V}_g}{\omega_s L_s} - \frac{L_m}{L_s} i_{dr} \right] \quad (19)$$

$$i_{qr} = -\frac{2L_s}{3V_g L_m} P_s; \quad i_{dr} = \frac{V_g}{L_m L_s \omega_s} - \frac{2}{3} \frac{Q_s L_s}{V_g L_m} \quad (20)$$

The above equations clearly show that, under the stator flux orientation, the active and reactive powers of the stator are decoupled and controlled via the rotor currents independently.

A. Real Time Control of DFIG

Once the parameters of the DFIG have been determined with tests conducted, the code composer studio (CCS) V7.0 software of the Texas Instrument (TI) [12] is used for programming and real time control of the actual machine using an F28069 microcontroller with MTL CBI0020N12IXFE Guasch Inverter [13] as shown in Fig. 7 and 8.

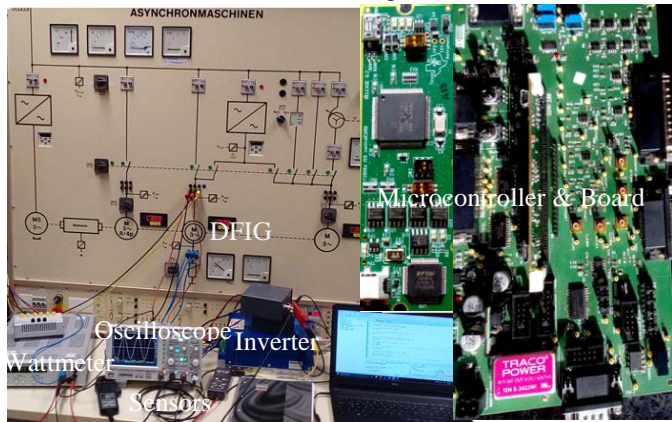


Fig. 7. DFIG under experimentation with other accessories

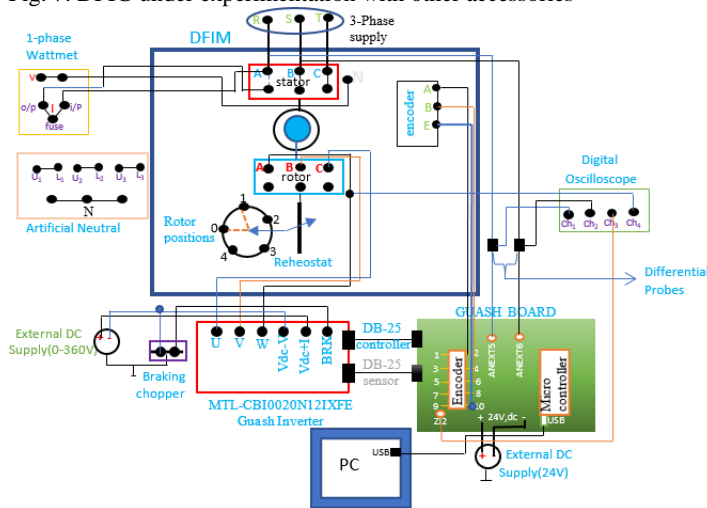


Fig. 8 Connection diagram of DFIG for controlling purpose

The Code Composer Studio in connection with the embedded programming language features a number of General Purpose Input/output (GPIO) ports, the Analog-to-Digital Conversion (ADC) process, interrupts, etc to execute a real time application through embedded code processors.

For instance, The ADC module described in this reference guide is a 12-bit ADC functioning of simultaneous sampling or sequential sampling modes with a full range analog input of 0 V to 3.3 V fixed, or VREFHI/VREFLO ratio metric and it has Up to 16-channel, multiplexed inputs. The ADC applications range from sampling a control signal for use in a digital notch filtering algorithm or using the ADC in a control feedback loop to monitor motor performance. Additionally, the ADC is useful in motor control applications because it allows for current sensing using a shunt resistor instead of an expensive current sensor [12], [14].

The external rotor dq currents are injected to the DFIG through the inverter and shaft for its active and reactive power control. The watch list window of CCS software is used to view parameters while controlling them. The DFIG rotor takes its reference from a microcontroller which is debugged by the program done in CCS and send proper switching signals to the IGBT drivers. The measured currents and voltages are feedback to the micro controller through the interfacing cables, after signal-conditioning and filtering. The Guash board developed based on TI's F28069 microcontroller is used for this purpose.

VII. EXPERIMENTAL AND SIMULATION RESULTS

A. Simulation Results

Based on the modelling of the machine done using MATLAB-Simulink as shown in Fig. 5, the simulation results are described in this section in order to compare the results.

As (20), at constant stator voltage, the required i_{dr} calculated for unity PF ($Q_s=0$) is 2.97A and similarly to control P_s at 1 kW; i_{qr} required is -2.4A. For $i_{dr}=0$, $Q_s=1258.3VAR$. The simulation results of Q_s controlled at 0 VAR and P_s at 1kW are shown in Fig. 9.

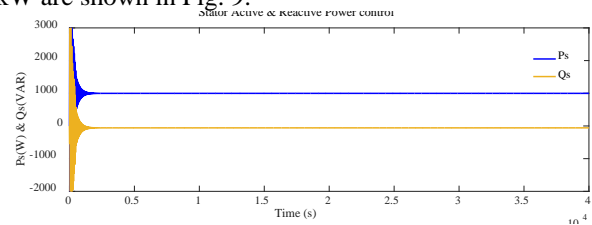


Fig. 9 Active and Reactive Power Control.

It can be seen that the Proportional Integral (PI) controller is able to tune P_s at 1kW but the reactive power is not exactly tuned to zero, but near. This seems that the large inductance and the assumption of neglecting the impact of stator resistance affected exact control of ensuring the unity PF.

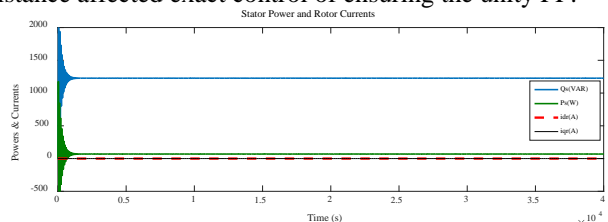


Fig. 10 Stator Active and reactive powers for zero dq rotor currents. The zero rotor dq currents are expected to control P_s at 0 and Q_s at 1258.3VAR. However, there are small deviations. That is, in the long run of the machine, the active power is seen to

be 72.5 W and the reactive power is 1254.14 VAR (Fig. 10). The same situation is observed in the experimentation and the reason seems to be the large value of the resistances, inductances and saturation of the machine. This can lead to a conclusion of saying that small sized DFIGs may be difficult to clearly resemble the larger machines in their performances. A step change of i_{qr} from 0 to -2.4A (P_s 0 to 1kW) and i_{dr} from 0 to 2.97A (Q_s 1258 to 0 VAR) simultaneously for their respective independent control is shown in Fig. 11 (a) and (b)

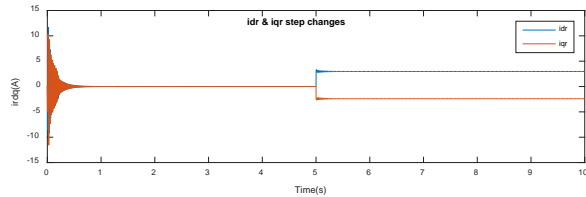


Fig. 11 (a) Step changes on rotor dq currents

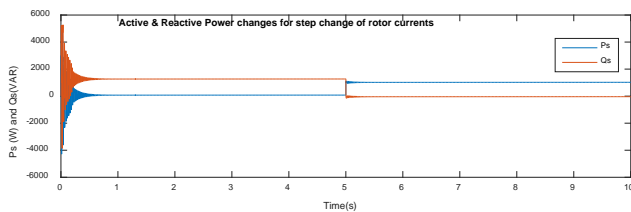


Fig. 11 (b) Response of dq rotor currents to step changes

A step change on i_{qr} resulted only on P_s and i_{dr} on Q_s as expected. However, there seen the small and insignificant effect on one another. The same effect was observed in laboratory experimentation. Therefore, the above figures can confirm an independent control of stator active and reactive power with their respective i_{qr} and i_{dr} currents.

A. Experimental Results

The machine is rated as 1kW, 400V rms stator, 127V rms rotor, 2.9A stator, 4.9A rotor, 0.71 power factor, 1500rpm synchronous speed, 1420 rpm rated speed, and 71% efficiency. The inverter is connected to the rotor of the machine with DC voltage of 250V. The results obtained by varying the rotor d and q currents in order to control the reactive and active power respectively are displayed in table VI.

No.	Rotor Current (A)		Ps (W)	Qs(VAR)	Udc (V)
	i_{dr}^*	i_{qr}^*			
1	0	0	468	1389	250
2	0.5	0	-495	1365	250
3	1	0	-486	1293	250
4	1.5	0	-477	1233	250
5	2	0	-450	1179	250
6	2.5	0	-441	1131	250
7	3	0	-414	1071	250
8	3.5	0	-405	999	250
9	4	0	-387	939	250
10	4.5	0	-378	903	250
11	5	0	-360	852	250
12	0	2	-1404	1314	499
13	0	2.5	-1656	1314	523.5
15	0	1	-72	261	250
16	0	2	-116	253	250
17	0	3	-162	251	250
18	0	4	-205	248	250
19	0	5	-248	243	250
20	0	6	-292	243	250
21	0	7	-337	243	250

22	0	8	-378	243	250
23	0	9	-428	243	250
24	1	1	-22	315	250
25	1	2	-66	316	250
26	1	3	-109	320	250
27	1	4	-150	320	250
28	1	5	-195	324	250

At a given machine torque and speed, it can be seen from the measurement results that the rotor d (i_{dr}^*) and q (i_{qr}^*) axis reference currents are independently controlling the reactive and active power of the DFIG. The change in i_{dr}^* is highly effected on Q_s whereas, i_{qr}^* on P_s as expected. However, there is also a small impact of i_{dr}^* on P_s and i_{qr}^* on Q_s . This can be one of the disadvantages and may be a problem of small sized DFIG that can affect exact independent control of P_s and Q_s . As per this experimentation, another limitation of small sized DFIG is its difficulty to exactly control Q_s for unity PF. It can also be seen in the table (No.12 & 13) that the change in DC bus voltage results with higher stator active and reactive power. The same situation can be seen with simulation. Thus, to increase the power generated from this DFIG, its dc bus voltage has to be increased.

VIII.CONCLUSION

As the torque increases, the efficiency of DFIG decreases and the input power at shaft increases. Therefore, the best efficiency can obtain in a generating mode is at lower rotor position (4) where it is 52%. At rated stator current, the power generated is around 600W at efficiency near 50%. It is possible to increase the generated power by increasing the torque, however, the situation result with increased stator current beyond rated value and the total loss. Therefore, it is suggested to operate a DFIM as a generator at lower rotor position where efficiency is better, the total loss is less for a given torque. The total loss increases as a change of rotor position in increased forward manner.

In case of a generator, to produce 1 kW at 71% rated efficiency, the input power required at the shaft will be: $P_{in}=1000/0.71=1.41kW$. The rated slip, s for the DFIG is -0.053. This is equivalent to 1579.5 rpm or 165.4rad/s. Thus, the torque required at the shaft is therefore $1410/165.4 = 8.5$ Nm. This torque is large compared with rated value and hence increasing the output power without having converter seems difficult. To use inverter drive for this machine at $n_m = 1579.5$ rpm, the output frequency, f_o of the drive for a DFIG with poles (p) = 4 is 53Hz that can be computed using $f_{inv}/f_o=n_m*P/120$. At 53 Hz, if the specified load capacity is 90%, thus the nominal torque of the emulator motor can be $8.5/0.90=9.5Nm$. Finally, the rated power of the required emulator motor is $9.5*1500*(2*\pi/60)=1.5$ kW. The better the efficiency had been, the lesser the size of emulator required. Thus a 1.5 kW squirrel-cage induction machine can be selected for the emulator function.

In this paper, the stator flux frame orientation with the assumption of ignoring the stator resistance considering its very low values for large megawatt machines was taken. However, on the contrary, the small sized DFIG conducted under this experimentation has large stator resistance (7.33Ω)

and its inductances are also large. This resulted in a problem of exactly controlling the zero-active power at zero i_{qr} and zero reactive power at 2.97A of i_{dr} even though they are getting controlled independently with their respective currents.

The test conducted proves the validity of DFIG as it has the capability of speed and power control over various torque ranges which allows the Wind Turbine to achieve the maximum wind energy extraction algorithm at a lower wind speed by designing appropriate control techniques.

REFERENCES

- [1] Sun, Tao, "Power Quality of Grid-Connected Wind Turbines with DFIG and Their Interaction with the Grid," Institut for Energiteknik, Aalborg Universitat, Aalborg, 2004
- [2] Martti Hokkanen, Heikki J. Salminen, Timo Vekara, "A Short Review of Models for Grid-Connected Doubly-Fed Variable Speed Wind Turbines," University of Vaasa, Finland, 2004.
- [3] Kearney, J., "Grid Voltage Unbalance and the Integration of DFIG's. Doctoral Thesis, Dublin Institute of Technology," 2013 doi: 10.21427/D7QK6V
- [4] Induction Machine, Chapter 6, www4.hcmut.edu.vn/~tcbinh/.../C4_Electric%20Machinery_C6.pdf [online]
- [5] Linder, Lehmann Brauer: Taschenbuch der Elektrotechnik und Elektronik.9.Auflage Hanser 2008, DFIM Manual
- [6] Gokaraju Rangaraju, Bachupally, Miyapur, Electrical Machine-II Laboratory Manual, HYDERABAD-500090, Institute of Engineering & Technology
- [7] G. Abad, J. Lo'pez, M. A. Rodriguez, L. Marroyo, and G. Iwanski, Doubly Fed Induction Machine: Modeling and Control for Wind Energy Generation, First Edi.2011, IEEE Press and John Wiley & Sons Ltd. Ch.4 & 7
- [8] Milkias Berhanu Tuka, Mengesha Mamo, "Performance Analysis of Grid Coupled Doubly Fed Induction Generator in a Wind Power System," WSEAS Transactions on Power Systems, Volume 12, 2017
- [9] Milkias Berhanu Tuka, Roberto Leidhold, Mengesha Mamo, "Modeling and Control of a Doubly Fed Induction Generator Using a Back-to-Back Converters in Grid Tied Wind Power System", 2017 IEEE PES-IAS PowerAfrica Conference
- [10] Haitham Abu-Rub, Mariusz Malinowski & etal, Power Electronics for Renewable Energy Systems, Transportation& Industrial Applications, 2014, IEEE Press and John Wiley & Sons Ltd. Ch.10
- [11] Gonzalo Abad, Power Electronics and Electric Drives for Traction Applications, First Edition, Ltd. Published 2017 by John Wiley & Sons, Ltd., pp.175
- [12]. Texas Instruments, <http://www.ti.com/lit/ug/spruh18f/spruh18f.pdf> [online]
- [13] MTL-CBI0060F12IXHF MT Series guasch board, https://dhh3yazwboecu.cloudfront.net/720/pdf/mtl-cbi0060f12ixhf_i.pdf [online]
- [14]. Hamid A. Toliyat, Steven G. Cambpel, DSP-Based Electromechanical Motion Control. CRC Press LLC 2004, pp. 257.